Report

Cell Reports

NCOA4 Deficiency Impairs Systemic Iron Homeostasis

Graphical Abstract

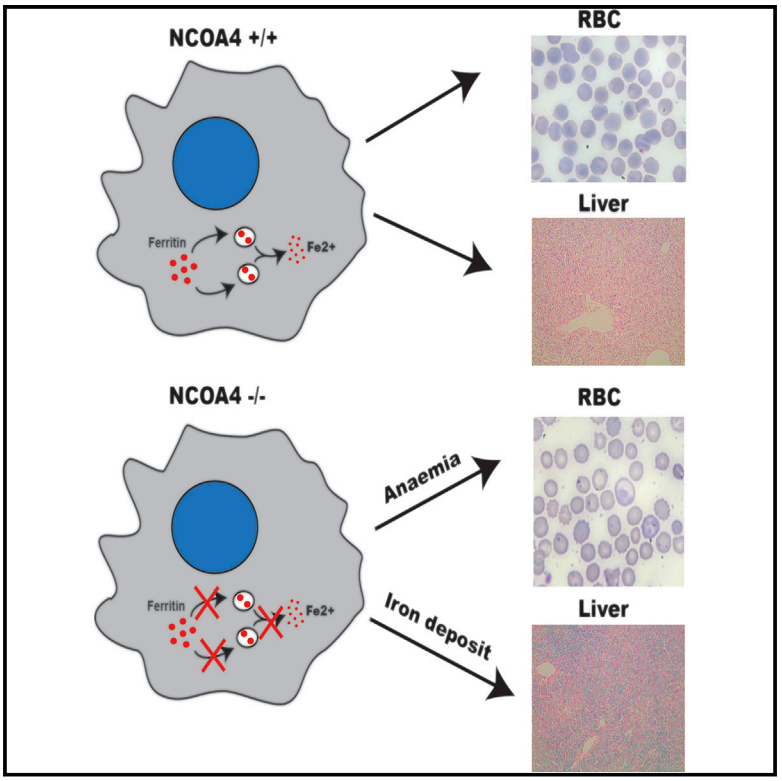

Highlights

- Genetic disruption of NCOA4 causes ferritin accumulation in tissues
- NCOA4 deficiency blocks iron mobilization from ferritin storage and induces anemia
- NCOA4-null mice are hypersensitive to iron overload

Authors

Roberto Bellelli, Giorgia Federico, Alessandro Matte', ..., Massimo Santoro, Lucia De Franceschi, Francesca Carlomagno

Correspondence

francesca.carlomagno@unina.it

In Brief

NCOA4 is crucial for autophagic ferritin degradation. Bellelli et al. find that genetic disruption of NCOA4 causes ferritin accumulation in tissues and defective iron mobilization from storage. NCOA4-null mice display impaired erythropoiesis associated with microcytic and hypochromic anemia, which is more pronounced in mice fed an iron-depleted diet.

Bellelli et al., 2016, Cell Reports *14*, 411–421
January 26, 2016
http://dx.doi.org/10.1016/j.celrep.2015.12.065

Cell Reports
Report

NCOA4 Deficiency Impairs Systemic Iron Homeostasis

Roberto Bellelli,[1,5] Giorgia Federico,[1] Alessandro Matte',[2] David Colecchia,[3] Achille Iolascon,[1,4] Mario Chiariello,[3] Massimo Santoro,[1] Lucia De Franceschi,[2] and Francesca Carlomagno[1,*]
[1]Dipartimento di Medicina Molecolare e Biotecnologie Mediche, Università degli Studi di Napoli Federico II, and Istituto di Endocrinologia ed Oncologia Sperimentale del Consiglio Nazionale delle Ricerche, 80131 Napoli, Italy
[2]Dipartimento di Medicina, Università degli Studi di Verona–Azienda Ospedaliera Universitaria Integrata Verona, 37134 Verona, Italy
[3]Istituto Toscano Tumori-Core Research Laboratory and Consiglio Nazionale delle Ricerche–Istituto di Fisiologia Clinica, 53100 Siena, Italy
[4]Centro di Ingegneria Genetica–Advanced Biotechnologies, 80145 Naples, Italy
[5]Present address: DNA Damage Response Laboratory, Clare Hall Laboratory, The Francis Crick Institute, South Mimms EN6 3LD, UK
*Correspondence: francesca.carlomagno@unina.it
http://dx.doi.org/10.1016/j.celrep.2015.12.065

SUMMARY

The cargo receptor NCOA4 mediates autophagic ferritin degradation. Here we show that NCOA4 deficiency in a knockout mouse model causes iron accumulation in the liver and spleen, increased levels of transferrin saturation, serum ferritin, and liver hepcidin, and decreased levels of duodenal ferroportin. Despite signs of iron overload, NCOA4-null mice had mild microcytic hypochromic anemia. Under an iron-deprived diet (2–3 mg/kg), mice failed to release iron from ferritin storage and developed severe microcytic hypochromic anemia and ineffective erythropoiesis associated with increased erythropoietin levels. When fed an iron-enriched diet (2 g/kg), mice died prematurely and showed signs of liver damage. Ferritin accumulated in primary embryonic fibroblasts from NCOA4-null mice consequent to impaired autophagic targeting. Adoptive expression of the NCOA4 COOH terminus (aa 239–614) restored this function. In conclusion, NCOA4 prevents iron accumulation and ensures efficient erythropoiesis, playing a central role in balancing iron levels in vivo.

INTRODUCTION

Iron is essential for oxygen transport, oxidation-reduction reactions, and metabolite synthesis (Andrews and Schmidt, 2007; Ganz and Nemeth, 2012). However, because of its high chemical reactivity and ability to generate reactive hydroxyl radicals through Fenton chemistry, iron concentration must be tightly controlled in tissues, cells, and blood (Papanikolaou and Pantopoulos, 2005). Notably, iron is stored in transport (transferrin) or deposit (ferritin) protein complexes to protect it from the deleterious effects of Fenton reactions. Ferritin is a ubiquitously expressed cytosolic multimeric protein complex constituted of 24 H- and L-polypeptide subunits that self-organize in different ratios in a tissue-dependent fashion and form a shell-like nanocage in which iron is stored. Each "cage" accommodates up to 4,500 iron atoms in the Fe(III) state (Arosio et al., 2009). Iron concentration in mammals is mainly regulated by a set of interlocking regulatory circuits involving hepcidin, hypoxia-inducible factor 2α (HIF2α), and iron regulatory proteins (IRPs) (Hentze et al., 2010).

Serum and tissue iron levels are principally regulated by iron absorption. Dietary heme iron is absorbed efficiently via membrane transport mechanisms that have yet to be fully characterized. Non-heme iron is transported into enterocytes by the divalent metal transporter 1 (DMT1), which is the apical transporter of iron ions. Most of the iron taken up is stored in ferritin and lost upon sloughing of senescent enterocytes. The basolateral transporter ferroportin (FNP) carries iron from enterocytes to the blood. Transferrin then transports iron to peripheral tissues via a receptor-mediated uptake process. Two transferrin receptors have been identified: a high-affinity, widely expressed receptor, transferrin receptor 1 (TfR1), which is required for cellular iron uptake, and a bone marrow/liver-specific low-affinity receptor, TfR2, which is mainly involved in the regulation of iron homeostasis in the liver and bone marrow (Nai et al., 2015).

The main hormone regulating intestinal iron uptake and release from splenic macrophages is hepcidin, whose production in the liver is controlled by serum iron concentrations, erythropoiesis, and inflammation. By promoting internalization and ubiquitin-mediated degradation of the iron transporter ferroportin I (Fnp1), hepcidin reduces iron absorption and its recycling from red blood cell breakdown. Hepcidin expression is regulated by systemic iron availability. Therefore, a high concentration of Fe(III)-saturated transferrin activates the TfR2 receptor in complex with the HFE (High Iron Fe) protein, which, in turn, promotes hepcidin transcription through the BMP/Smad and, probably, the extracellular signal-related kinase (ERK)/mitogen-activated protein kinase (MAPK) signaling pathways. In addition, increased tissue iron activates the Smad pathway by increasing BMP6 production. By binding BMP receptors in complex with the hemojuvelin protein, BMP6 activates the Smad pathway, leading to increased hepcidin production (Babitt et al., 2006). The expression of iron transporters in the duodenum is also regulated by the transcription factor HIF2α, which binds to hypoxia-responsive elements in the promoters of ferroportin and DMT1 (Mastrogiannaki et al., 2009).

Dysregulation of hepcidin production, because of a plethora of genetic defects of iron homeostasis, causes iron overload and results in a systemic disease known as "hereditary

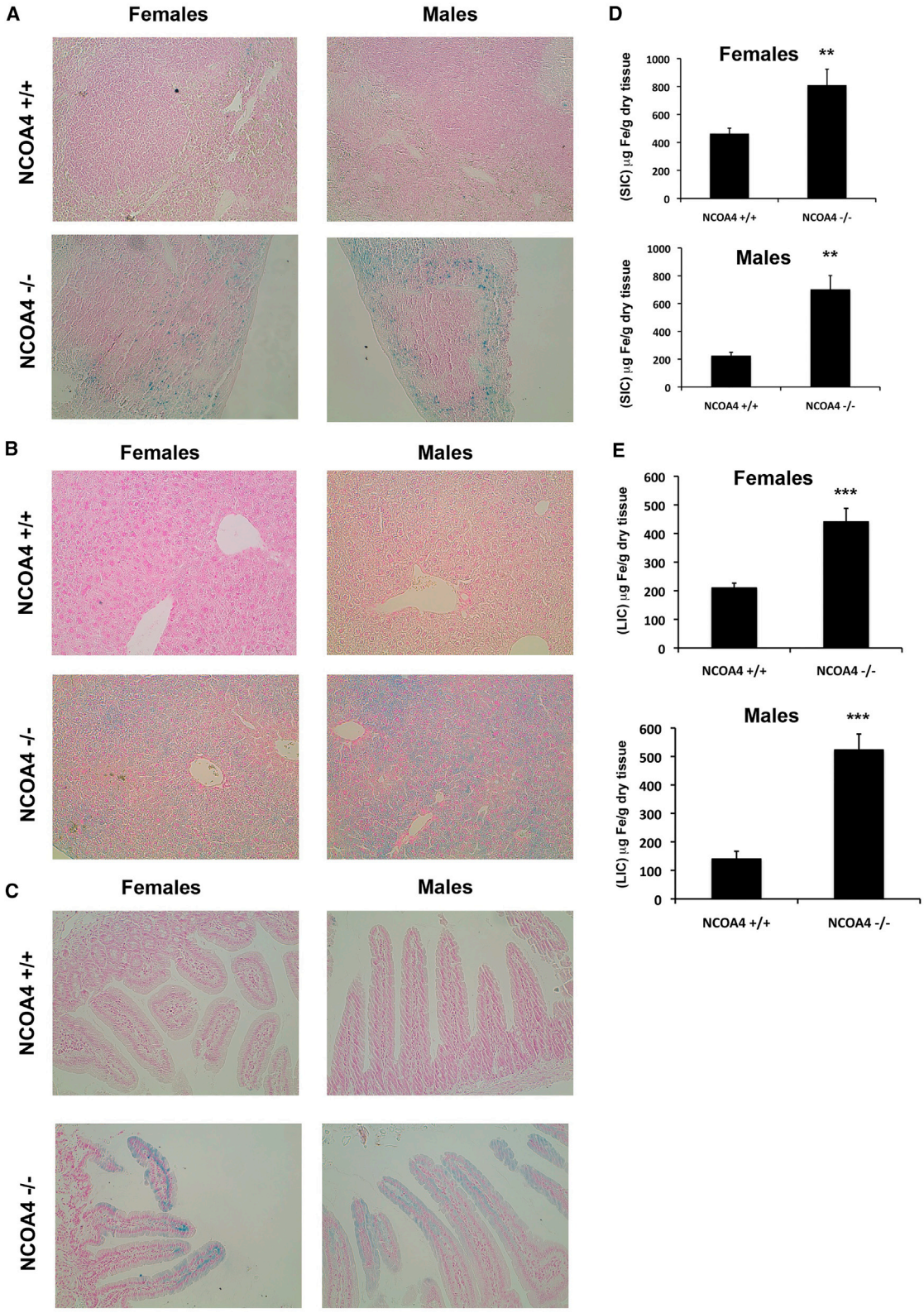

Figure 1. Increased Iron Accumulation in NCOA4-Null Mouse Liver, Spleen, and Duodenum

(A) Representative Perls' Prussian blue staining of WT (+/+) and NCOA4-null (−/−) spleen sections from 2-month-old female and male mice. Magnification, ×20.

(B) Representative Perls' Prussian blue staining of WT (+/+) and NCOA4-null (−/−) liver sections from 2-month-old female and male mice. Magnification, ×20.

(legend continued on next page)

hemochromatosis,'' which is characterized by tissue iron accumulation, iron-mediated injury, and organ dysfunction (Fleming and Ponka, 2012). Mouse models of hereditary hemochromatosis correctly recapitulate various human diseases (Hentze et al., 2010).

To avoid iron overload, cells shelter iron in ferritin. Consequently, a high concentration of iron promotes the translation of ferritin subunits by inactivating the iron regulatory protein (IRP)/iron-responsive element (IRE) machinery (Zhang et al., 2014; Zhao et al., 2013). On the contrary, under conditions of iron deficiency or increased iron requirement, mobilization of iron from ferritin deposits is supported via autophagy (''ferritinophagy'') (Mancias et al., 2014).

Protein NCOA4, which interacts with and co-activates several nuclear hormone receptors and controls DNA replication origin activation, thereby preserving genome stability (Bellelli et al., 2014; Heinlein et al., 1999; Lanzino et al., 2005; Yeh and Chang, 1996), has been identified recently as a crucial player in ferritinophagy (Dowdle et al., 2014; Mancias et al., 2014). Therefore, NCOA4 functions as a cargo receptor that, by interacting with ferritin, promotes its transport to autophagosomes via interaction with ATG8-like proteins such as GABARAP and GABARAPL1, sustaining iron release under both basal and iron starvation conditions. Inactivation of NCOA4 in cells causes an increase in ferritin deposits (Dowdle et al., 2014; Mancias et al., 2014).

The aim of this study was to explore the involvement of NCOA4 in ferritinophagy in vivo using an NCOA4$^{-/-}$ mouse model. To determine the role of NCOA4 in maintaining in vivo iron homeostasis, we exposed NCOA4$^{-/-}$ mice to a high- or low-iron diet. We also evaluated the ability of mouse embryonic fibroblasts (MEFs) from NCOA4-null mice to target ferritin to autophagolysosomal digestion under basal and iron-depleted conditions.

RESULTS

NCOA4-Null Animals Display Ferritin Accumulation

To determine whether ferritin deposits were enhanced in NCOA4-null animals as a consequence of impaired ferritinophagy, we analyzed protein extracts from the liver, spleen, duodenum, bone marrow, and kidney of NCOA4$^{-/-}$ and wild-type (WT) animals by western blotting. As shown in Figure S1, ferritin content (FTH1) was significantly higher in NCOA4-null mice than in WT mice in all analyzed tissues. Perls' Prussian blue staining of the liver, spleen, and duodenum confirmed this finding (Figures 1A–1C). Consistently, iron concentrations were significantly higher in the spleens and livers of NCOA4-null than in WT animals (Figures 1D and 1E).

NCOA4-Null Animals Display Increased Serum Iron, Transferrin Saturation, and Hepcidin Upregulation

The percentages of transferrin saturation and serum ferritin levels were increased slightly but significantly in NCOA4-null versus WT animals (Figures S2A and S2B). This indicates that tissue iron in the knockout animals is in equilibrium with circulating iron. Generally, increased transferrin saturation activates a signaling pathway in hepatocytes that leads to increased hepcidin gene (HAMP) transcription to reduce iron absorption. At real-time PCR, HAMP mRNA expression was 2-fold higher in NCOA4-null livers versus WT tissues (Figure S2C). Western blotting with anti-phospho Smad1/5/8 antibody did not show increased phosphorylation of Smad proteins in the livers of knockout animals (data not shown) but, rather, increased phosphorylation of proteins ERK1/2 (Figure S2D). Consistent with increased HAMP expression, FNP protein expression was lower in the duodeni of NCOA4-null mice than in those of WT animals (Figure S3A). NCOA4 deficiency did not significantly affect the expression of protein HIF2α or of FPN mRNA in duodenum enterocytes (Figures S3B and S3C). Furthermore, IRP2 protein levels were not increased in NCOA4-null mouse livers. This finding strongly suggests that, notwithstanding the increase in ferritin content in various tissues, the IRP/IRE and HIF2 systems, which are mainly influenced by alteration of labile intracellular iron, were not affected (Figure S3D). Accordingly, levels of TfR1 mRNA (containing multiple IRE elements in the 3′ UTR) and protein were similar in the livers of NCOA4-null and WT mice (Figures S3D and S3E), as was FTH1 mRNA expression (Figure S3E). In summary, NCOA4-null mice, despite their ability to activate the hepcidin/ferroportin pathway, accumulated iron in tissues. Notably, no gender differences were observed.

NCOA4-Null Mice Display Hypochromic Microcytic Anemia that Is Exacerbated by a Low Dietary Iron Intake

To determine whether the failure of NCOA4-null mice to degrade ferritin and mobilize stored iron affects erythropoiesis, we evaluated red blood parameters in NCOA4-null and WT mice at baseline and after prolonged exposure to a low-iron diet; namely, for 5 and 7 months. As shown in Table 1, at baseline, compared with WT animals, NCOA4-null mice had significantly lower values of hematocrit, hemoglobin, mean corpuscular volume, and mean corpuscular hemoglobin, a condition compatible with microcytic anemia.

To examine defective erythropoiesis in greater detail, we analyzed ferritin deposits by western blotting in knockout and WT animals fed an iron-poor diet (2–3 mg/kg) for 5 months, which is sufficient time to allow iron mobilization from ferritin. As shown in Figures 2A and S4A, although, after 5 months of iron depletion, ferritin deposits were completely exhausted in WT livers and spleens, a large amount of ferritin was still present in NCOA4-null mice. Indeed, liver and spleen iron content was significantly higher in knockout than in WT animals (Figure 2B). On the contrary, serum iron and transferrin saturation, which, under a normal diet, were higher in NCOA4-null than in WT animals (Figure S2A; data not shown), were significantly lower under a low-iron diet in NCOA4-null than in WT animals (Figure 2C).

(C) Representative Perls' Prussian blue staining of WT (+/+) and NCOA4-null (−/−) duodenum sections from 2-month-old female and male mice. Magnification, ×20.

(D) Splenic non-heme iron content (SIC) of WT (+/+) and NCOA4-null (−/−) female and male mice. Data are shown as mean ± SD from 4–5 independent samples.

(E) Liver non-heme iron content (LIC) of WT (+/+) and NCOA4-null (−/−) female and male mice. Data are shown as mean ± SD from 4–5 independent samples.

**$p < 0.01$, ***$p < 0.001$. See also Figures S1, S2, and S3.

Table 1. Hematological Parameters and Red Cell Indices in NCOA4$^{+/+}$ and NCOA4$^{-/-}$ MICE under Standard and Iron-Deficient Diets

			Iron-Deficient Diet			
	Baseline		5 Months		7 Months	
	NCOA4$^{+/+}$ Mice (n = 6)	NCOA4$^{-/-}$ Mice (n = 6)	NCOA4$^{+/+}$ Mice (n = 6)	NCOA4$^{-/-}$ Mice (n = 6)	NCOA4$^{+/+}$ Mice (n = 3)	NCOA4$^{-/-}$ Mice (n = 4)
Hct (%)	45.8 ± 1.1	42.2 ± 1.3*	36.7 ± 1.3°	28.6 ± 2.8°*	36.0 ± 0.6°	28.8 ± 3.3°*
Hb (g/dl)	15.1 ± 0.2	12.7 ± 0.6*	11.8 ± 0.3°	8.8 ± 1.7°*	11.0 ± 0.5°	8.0 ± 1.8°*
MCV (fl)	51.7 ± 0.5	46.3 ± 3.05*	47.5 ± 1.5°	38.5 ± 4.1°*	43.7 ± 2.7°	36.5 ± 2.4°*
MCH (pg)	16.3 ± 0.8	15.6 ± 0.2*	15.4 ± 1.2	10.3 ± 0.9°*	14.1 ± 1.3°	10.4 ± 1.5°*
MCHC (g/dl)	27.6 ± 0.4	28.2 ± 0.5	27.5 ± 0.3	26.1 ± 0.9°*	26.7 ± 0.6	26.7 ± 0.6°
CH (pg)	14.9 ± 0.3	13.0 ± 0.5	13.1 ± 0.6°	9.92 ± 0.9°*	10.12 ± 0.4°	9.57 ± 0.86°
RDW (%)	12.6 ± 0.5	15.1 ± 2.5	13.1 ± 0.7	23.4 ± 4.0°*	30.12 ± 6.1°	28 ± 7.3°*
Retics (10^3cell/μl)	498 ± 84	488 ± 170	419 ± 98	60 ± 2.8°*	41 ± 15°	52 ± 0.8°
MCVr (fl)	55.2 ± 0.4	51 ± 1.84*	53.6 ± 1.9°	48.5 ± 5.4°*	41.6 ± 5°	40.2 ± 2.8°
CHr (pg)	14.7+0.8	13.8 ± 1.1	13.45 ± 1.5	11.0 ± 0.78°*	13.5 ± 1.1	9.05 ± 1.3°*

Hct, hematocrit; Hb, hemoglobin; MCV, mean corpuscular volume; MCH, mean corpuscular hemoglobin; MCHC, mean corpuscular hemoglobin concentration; CH, hemoglobin concentration; RDW, red cell distribution width; Retics, reticulocytes; MCVr, reticulocyte mean corpuscular volume; CHr, reticulocyte hemoglobin concentration. *$p < 0.05$ compared with WT mice; °$p < 0.05$ compared with baseline.

Consistent with this finding, hepcidin mRNA levels were suppressed completely in NCOA4$^{-/-}$ livers, whereas ferroportin protein expression was increased significantly in spleen macrophages despite the accumulation of ferritin in the spleen (Figures S4B and S4C).

These data strongly indicated that NCOA4-null animals were unable to mobilize iron from ferritin deposits when subjected to an iron depletion regimen. Therefore, we explored the effects of a low-iron diet on red cells and erythropoiesis. After 5 months of a low-iron diet, NCOA4-null mice developed severe hypochromic microcytic hyporegenerative anemia and anisopoikilocytosis (Figure 2D). This was associated with significantly lower values of hemocrit, hemoglobin, mean corpuscular volume, mean corpuscular hemoglobin, mean corpuscular hemoglobin concentration, hemoglobin concentration, reticulocytes, and a significantly lower reticulocyte mean corpuscular volume in NCOA4-null than in WT mice (Table 1). After 7 months of a low-iron diet, the hypochromic microcytic anemia became more severe in NCOA4$^{-/-}$ mice, and the reticulocyte hemoglobin concentration was significantly lower than in WT mice. These results indicate a severe reduction in the availability of iron required for cell hemoglobinization (Figure 2D; Table 1). Notably, WT mice developed only mild hypochromic anemia after 5 months of a low-iron diet and severe microcytic and hypo-regenerative anemia after 7 months of a low-iron diet (Figure 2D; Table 1). Consistently, erythropoietin expression was significantly higher in NCOA4-null than in WT animals after both 5 and 7 months of a low-iron diet (Figure 2E).

To characterize the different forms of anemia, we explored NCOA4-null mice erythropoiesis using a recently developed flow cytometry strategy. This strategy combines CD44 and TER119 positivity with cell size to quantify terminal erythroid differentiation by sorting bone marrow erythroid precursors at each distinct developmental stage (population I, pro-erythroblasts; population II, basophilic erythroblasts; population III, polychromatic erythroblasts; population IV, orthochromatic erythroblasts) (Liu et al., 2013). As shown in Figure 2F, after 7 months of a low-iron diet, the decrease in Fsc^{high} CD44^{+} Ter119^{+} cells was more pronounced in NCOA4-null mice than in WT animals. The process of terminal erythroid differentiation did not differ substantially between untreated NCOA4-null and WT mouse bone marrow (Figure S4D). However, at the same time point, orthochromatic erythroblasts were significantly fewer in NCOA4-null mice than in WT animals (Figure 2G). The decrease in orthochromatic erythroblasts was associated with significantly higher amounts of apoptotic orthochromatic erythroblasts in NCOA4-null mice than in WT mice already after 5 months of diet (Figure S4E). The number of apoptotic orthochromatic erythroblasts increased in WT mice only after 7 months of a low-iron diet (data not shown). Overall, these data indicate that genetic inactivation of NCOA4 impairs the mobilization of iron from liver and spleen deposits, thereby promoting anemia, particularly under conditions of iron deficiency.

NCOA4-Null Animals Are Hypersensitive to an Iron-Rich Diet

Increased iron deposits in NCOA4-null mice tissues (Figure 1; Figure S1) suggested that these animals might poorly tolerate an increased iron intake. To explore this possibility, knockout and WT animals were fed chow containing 2 g/kg iron. After 15 days of a hyperferric diet, both FTH1 protein levels and iron content were higher in NCOA4$^{-/-}$ liver extracts than in the WT counterparts (Figures 3A and 3B). Furthermore, Perls' Prussian blue staining was more intense and diffuse in NCOA4$^{-/-}$ than in WT livers (Figure 3C). Saturation of ferritin deposits presumably leads to an increase of free iron concentration and Fenton reaction-mediated oxidative stress, which causes hepatocyte damage and, eventually, cell death. Hepatocytes react to oxidative stress by activating the transcription of scavenger proteins such as superoxide dismutase (SOD) and glutathione peroxidase (GPx) (Vanoaica et al., 2010). Consistent with an increased

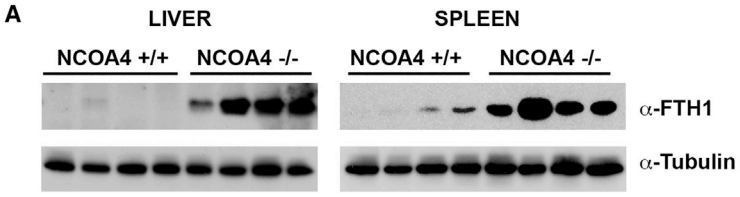

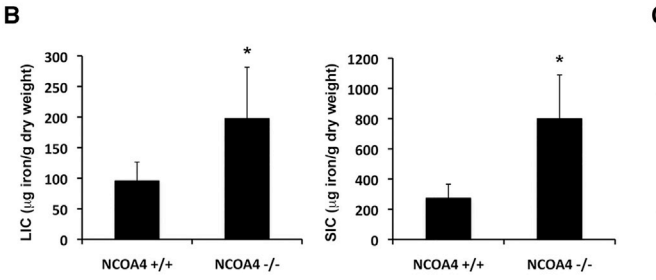

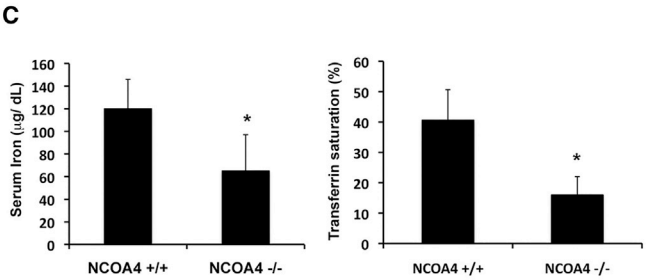

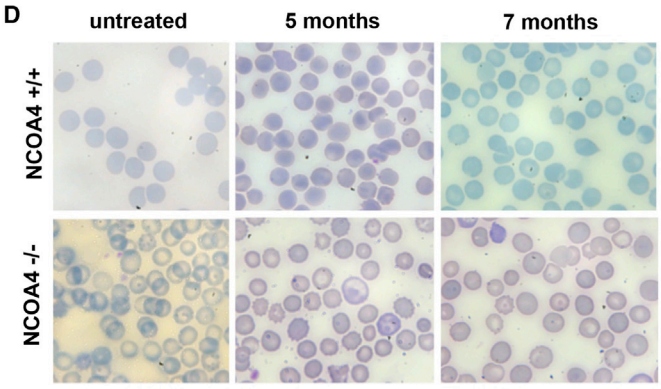

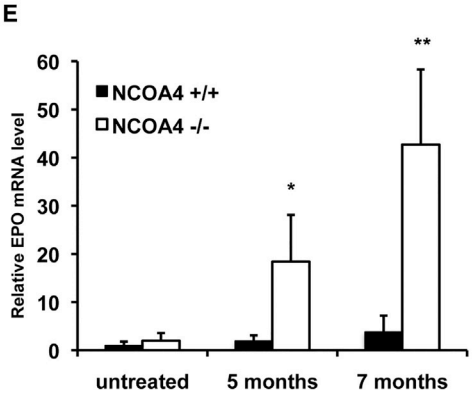

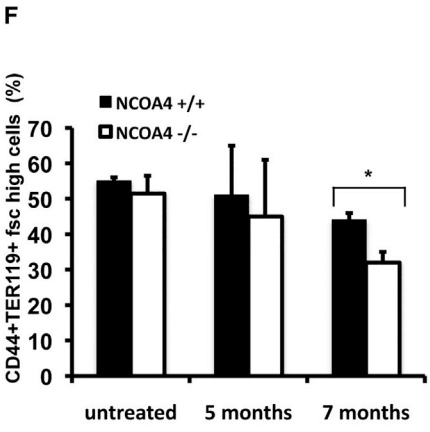

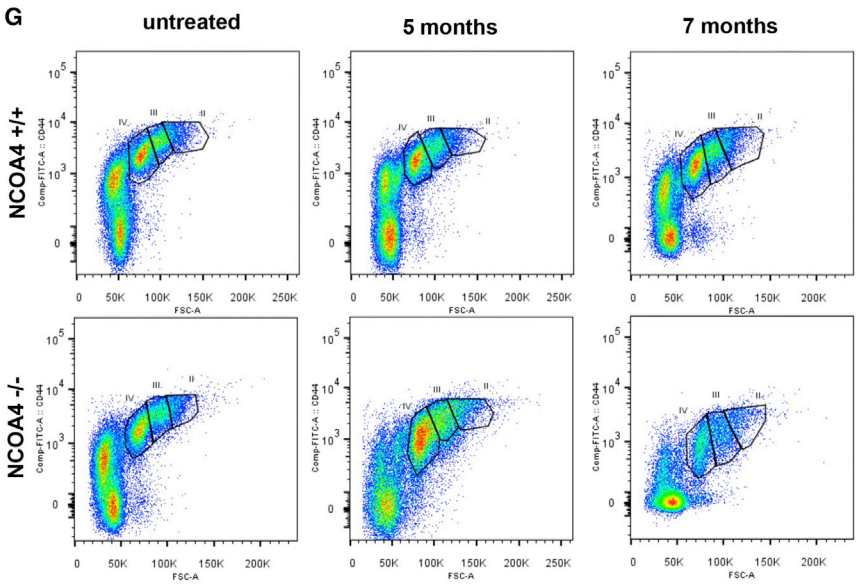

(legend on next page)

reactive oxygen species (ROS) concentration in NCOA4$^{-/-}$ hepatocytes, SOD and GPx gene expression was significantly higher in NCOA4$^{-/-}$ than in WT hepatocytes (Figure 3D). To verify hepatocyte cell damage, we measured the concentrations of alanine and aspartate liver transferases (ALT and AST, respectively), which are considered a bona fide measure of liver damage, in NCOA4-null and WT animals after 1 month of a hyperferric diet. As shown in Figure 3E, both enzymes were significantly higher in NCOA4-null animals than in WT mice, indicating precocious hepatic damage in knockout animals. Indeed, after 2 months of a hyperferric diet, fatty degeneration, which is a sign of hepato-steatosis, was more pronounced in livers of NCOA4-null than in those of WT mice, indicating more severe tissue damage in the former animals (Figure 3F). Finally, NCOA4-null animals started to die 75 days after diet onset, whereas WT animals started to die only after 100 days. Mean survival was 89 days in NCOA4-null animals and 104 days in WT animals, which corresponds to a 15% reduction in the mean survival of NCOA4-null mice (Figure 3G).

NCOA4-Null Mouse Embryonic Fibroblasts Display Impaired Ferritinophagy

To functionally verify the above results, we immortalized MEFs from NCOA4-null and WT mice in culture and evaluated their ability to target ferritin to autophagolysosomal digestion under both basal and iron-depleted conditions. Initially, we studied the intracellular localization of ferritin by confocal immunofluorescence analysis of MEFs treated with chloroquine, which, by inhibiting autophagosome-lysosome fusion and lysosomal protein degradation, reveals proteins contained in autophagosomes (Klionsky et al., 2012). As shown in Figure 4A, ferritin co-localized with LC3B-positive autophagosomes in WT MEFs, whereas ferritin was dispersed in the cytoplasm of NCOA4-null cells. In addition, western blotting showed that ferritin accumulation at steady-state was higher in NCOA4-null MEFs than in WT MEFs, which suggests reduced targeting of ferritin to autophagy in the former animals (Figure 4B). Consistently, when treated with ferric ammonium citrate (to induce iron accumulation in ferritin deposits) followed by the iron chelator deferoxamine (to promote iron release by ferritin digestion), WT MEFs rapidly degraded more than 80% of ferritin within 6 hr, whereas the kinetics of ferritin digestion in NCOA4-null cells was much slower, with more than 50% of deposits being present 9 hr after treatment (Figure 4C).

NCOA4 promotes ferritinophagy by directly interacting with the ATG8-like proteins GABARAP and GABARAPL1, localized on the membrane of autophagic vesicles, but not with the ATG8-like protein LC3B (Mancias et al., 2014). To study the molecular determinants of NCOA4-mediated interaction with the autophagosome receptors, we performed pull-down experiments with HEK293 cell extracts exogenously expressing the myc-tagged full-length NCOA4, the hemagglutinin (HA)-tagged N-terminal (N) NCOA4 (1–238 amino acids [aa]), and the C-terminal (C) NCOA4 (239–618 aa) using glutathione S-transferase (GST)-fused recombinant proteins of the ATG8-like polypeptides LC3B, GABARAP, and GABARAPL1. As reported by Mancias et al. (2014), full-length NCOA4 was pulled down by GABARAP and GABARAPL1 but not by LC3B (Figure S5A). Interestingly, only the NCOA4 (C), but not the NCOA4 (N) fragment, was able to bind to both GST-GABARAP and GST-GABARAPL1 (Figure S5B). To identify the NCOA4 protein domain responsible for interaction with ferritin, we then performed pull-down experiments using NUS-NCOA4, NUS-NCOA4 (C), and NUS-NCOA4 (N) recombinant proteins together with the isolated NUS moiety. As shown in Figure S5C, both NUS-NCOA4 and NUS-NCOA4 (C) were able to pull down ferritin whereas NUS and NUS-NCOA4 (N) were not, suggesting that the C-terminal fragment of NCOA4 protein mediates interaction with both ferritin and the autophagosomal machinery.

Confocal microscopy of EGFP-GABARAP- and EGFP-GABARAPL1-transfected HeLa cells confirmed that, like the full-length NCOA4 protein, the NCOA4 COOH-terminal fragment was able to localize to autophagosomes whereas the NCOA4 NH2-terminal fragment was not (Figures S5D and S5E). Finally, like the WT protein, the NCOA4 COOH-terminal fragment was able to complement NCOA4-null MEF-impaired ferritinophagy whereas the NCOA4 N-terminal fragment was not (Figure 4D). In summary, these data indicate that the NCOA4 COOH-terminal fragment is necessary and sufficient for interaction with both ferritin and autophagosomes and for promoting ferritinophagy.

Figure 2. Defective Iron Release from Ferritin Storage and Impaired Erythropoiesis in NCOA4-Null Mice

(A) Western blot analysis of FTH1 protein levels from WT (+/+) and NCOA4-null (−/−) female mice fed an iron-depleted diet for 5 months (2–3 mg Fe/kg of food). Tubulin was used as loading control.

(B) Left: LIC of WT (+/+) and NCOA4-null (−/−) mice fed an iron-depleted diet (5 months). Right: SIC of WT (+/+) and NCOA4-null (−/−) mice fed an iron-depleted diet (5 months). Data are shown as mean ± SD of 4 independent samples (*$p < 0.05$).

(C) Left: serum iron concentration of WT (+/+) and NCOA4-null (−/−) mice fed an iron-depleted diet (5 months). Right: percentage of transferrin saturation of WT (+/+) and NCOA4-null (−/−) mice fed an iron-depleted diet (5 months). Data are shown as mean ± SD of 4 independent samples (*$p < 0.05$).

(D) Representative May-Grünwald-Giemsa staining of peripheral blood smears from WT (+/+) and NCOA4-null (−/−) mice subjected or not subjected for 5 or 7 months to a low-iron (2–3 mg Fe/kg of food) diet. Original magnification, ×40.

(E) Relative erythropoietin mRNA expression in kidneys from WT (+/+) and NCOA4-null (−/−) mice under basal conditions (+/+, two females and five males; −/−, two females and six males) and after 5 months (+/+, three females; −/−, three females) or 7 months (+/+, three males; −/−, four males) of an iron-deficient diet (*$p < 0.05$, **$p < 0.01$).

(F) Percentage of CD44^{+}/CD119^{+}/fsc-high bone marrow cells in WT (+/+) and NCOA4-null (−/−) mice under basal conditions (+/+, three females and three males; −/−, three females and three males) and after 5 months (+/+, three females and three males; −/−, three females and three males) or 7 months (+/+, three males; −/−, four males) of iron-deficient diet (*$p < 0.05$).

(G) Flow cytometry analysis combining CD44, CD119, and cell size as markers to sort erythroid precursors at each distinct developmental stage (population I, proerythroblasts; population II, basophilic erythroblasts; population III, polychromatic erythroblasts; population IV, orthochromatic erythroblasts).

See also Figure S4.

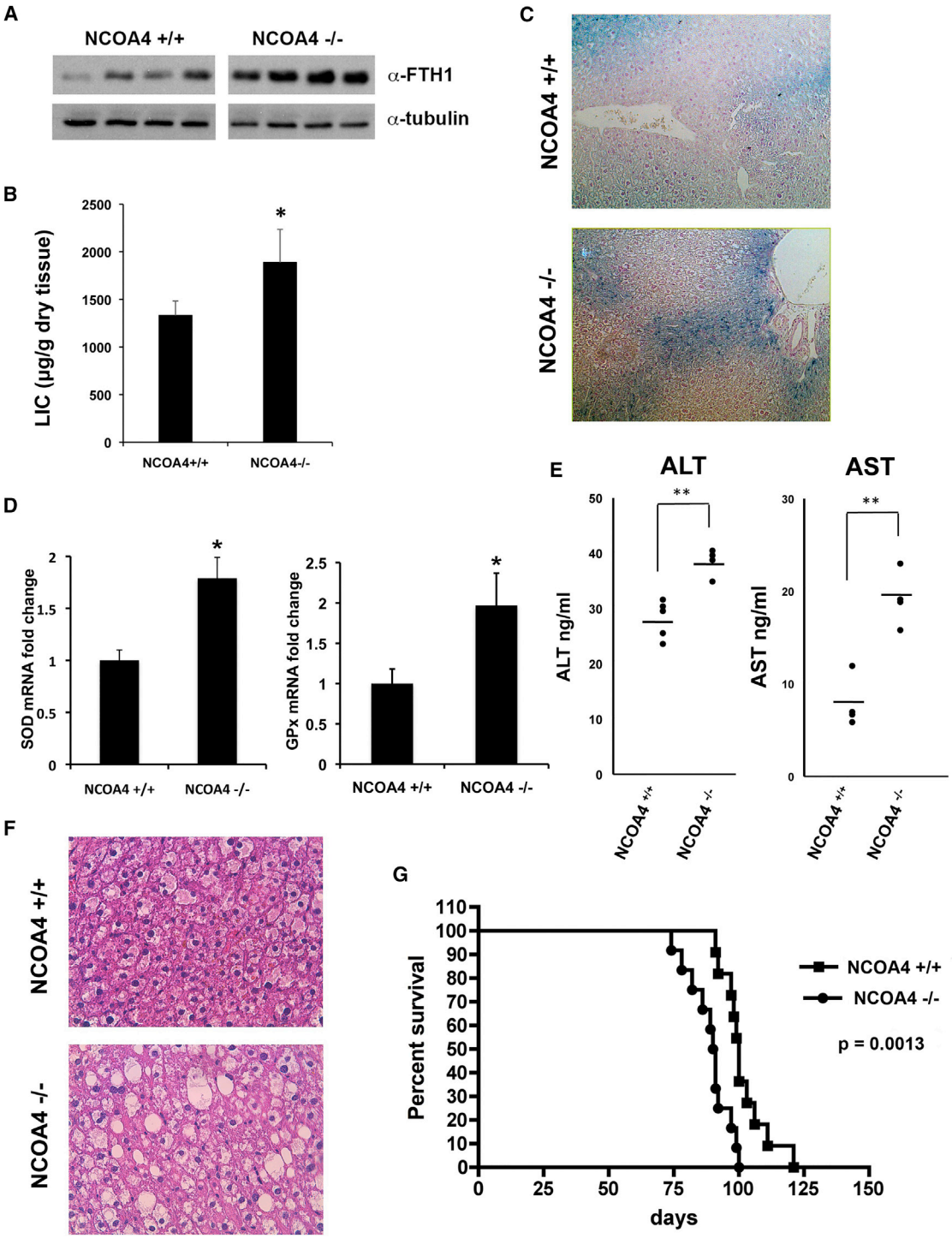

Figure 3. Iron Overload Leads to Liver Damage and Reduces Survival of NCOA4-Null Mice

(A) Western blot analysis of FTH1 protein levels from WT (+/+) and NCOA4-null (−/−) mice fed an iron-rich diet for 15 days. Tubulin was used as a loading control. The samples were run on the same SDS-PAGE gel and transferred and hybridized on the same filter. They were mounted separately because we did not include unrelated samples that were loaded in the central wells of the gel.

(B) LIC of WT (+/+) and NCOA4-null (−/−) mice subjected to a high-iron diet for 15 days. Data are shown as mean ± SD from 4–5 independent samples. (*$p < 0.05$).

(C) Representative Perls' Prussian blue staining of WT (+/+) and NCOA4-null (−/−) liver sections from mice subjected to an iron-rich diet for 15 days. Magnification, ×20.

(D) Real-time PCR of SOD and GPx mRNA expression in livers from $NCOA4^{+/+}$ and $NCOA4^{-/-}$ mice subjected to a hyperferric diet for 1 month (*$p < 0.05$).

(legend continued on next page)

DISCUSSION

NCOA4 promotes autophagic ferritin degradation to mobilize iron from deposits under both normal and iron-depleted conditions in vitro (Mancias et al., 2014; Dowdle et al., 2014). Here we describe the role of NCOA4 in controlling iron homeostasis in vivo. Loss of NCOA4 function induced ferritin accumulation in all analyzed tissues. Therefore, liver and spleen iron content were significantly higher in knockout than in WT animals. Transferrin saturation and serum ferritin were significantly higher in knockout than in WT animals and were probably sustained by iron overload in tissues. This phenotype resembles that described by Iolascon et al. (2006) in a patient carrying genetic inactivation of the DMT1 gene and displaying hepatic iron overload, microcytic hypochromic anemia, and increased levels of transferrin saturation. Increased transferrin saturation in NCOA4-null mice presumably leads to increased hepcidin mRNA levels, possibly consequent to activation of the TfR2/HFE receptor complex, as suggested by the increased activation of the ERK pathway. In turn, increased hepcidin reduces FNP levels in duodenal enterocytes, limiting iron absorption. Such a compensating mechanism could be responsible for the mild nature of the iron overload phenotype displayed by NCOA4-null animals.

Despite their ability to produce hepcidin to compensate for tissue iron overload, NCOA4-null mice subjected to a high iron content diet displayed early signs of steatohepatitis, as witnessed by increased serum transaminase levels and increased liver fat deposition. The low survival time of knockout animals on a hyperferric diet is probably due to the enhanced levels of basal tissue iron, which may accelerate saturation of the detoxification pathways that protect cells against the deleterious effects of iron-dependent oxidative reactions. All previous mouse models of hereditary hemochromatosis are based on the absence of either hepcidin production or resistance to hepcidin action, whereas NCOA4-null animals are fully competent for hepcidin production and activity on duodenal ferroportin, as shown by decreased levels of ferroportin in NCOA4-null duodenal enterocytes (Figure S3A). Therefore, to our knowledge, NCOA4-null mice represent the first example of a hepcidin-independent model of tissue hemochromatosis. Although no NCOA4 mutations have yet been identified in patients, this gene might represent a candidate modifier of iron overload diseases, which are often associated with a variable phenotype and incomplete penetrance (Fleming and Ponka, 2012).

Our data also indicate that impaired NCOA4 function predisposes to iron deficiency anemia, especially in animals fed a low-iron diet. Various observations have implicated NCOA4 in erythropoiesis. For instance, NCOA4 is highly expressed in erythroid precursors (https://genome-euro.ucsc.edu/). It is also particularly expressed during erythropoiesis in zebrafish mutants harboring defects of specific stages of hematopoiesis (Weber et al., 2005). Lastly, Mancias et al. (2015) have shown recently that NCOA4 plays an essential role in erythropoiesis in zebrafish embryos and cultured erythrocytes. Our mouse model suggests that the absence of NCOA4 also favors anemia in adult animals and under unstressed erythropoietic conditions. In fact, the use of iron deposits is impaired in NCOA4-null animals, inducing a peculiar mild hypochromic microcytic anemia associated with increased tissue iron content and transferrin saturation. These data suggest that, during erythroblast development, when liberated from transferrin, iron is, at least in part, stored intermediately in ferritin. In the absence of NCOA4, use of the ferritin-bound iron pool would be limited. Under hypoferric conditions, NCOA4-null mice develop severe anemia because of a remarkable reduction in circulating iron and ineffective erythropoiesis associated with reduction of the erythroid mass and increased apoptosis of orthochromatic erythroblasts. In this view, NCOA4 might also represent a modifier of genetic predisposition to iron deficiency.

Besides controlling ferritinophagy, NCOA4 has also been described as a coactivator of nuclear receptors and, in particular, of androgen receptor-, estrogen receptor-, and peroxisome proliferator-activating receptor γ (Heinlein et al., 1999; Yeh and Chang, 1996). We showed recently that NCOA4 controls DNA replication origin activation by inhibiting the processive helicase of the replication fork; i.e., the MCM2-7 complex, via its NH2-terminal portion (Bellelli et al., 2014). Interestingly, in their proteomic screening for NCOA4-interacting polypeptides, Mancias et al. (2014) and Dowdle et al. (2014) identified several MCM2-7 complex components. Moreover, the protein HERC2, which is an important player in the DNA damage response and in DNA replication origin activation, has been found to bind NCOA4 in an iron-dependent manner, promoting its ubiquitination and proteosomal degradation (Bekker-Jensen et al., 2010; Izawa et al., 2011; Mancias et al., 2015).

In structure-function experiments, we observed that the COOH-terminal portion of NCOA4 was necessary and sufficient to interact with both ferritin and ATG8-like proteins and that it was also able to complement ferritinophagy in NCOA4-null MEFs. This is in line with Mancias et al. (2015), who recently demonstrated that NCOA4 binding to FTH requires residues I489 and W497, both of which are contained in the COOH-terminal portion of the protein. Our data also indicate that the NCOA4 oligomerization motif contained within the protein's NH2-terminal portion is dispensable for ferritinophagy. Therefore, the two NCOA4 functions are separated structurally: the NH2-terminal portion interacts with DNA replication machinery, and the COOH-terminal portion interacts with the players crucial for ferritinophagy. Whether and how these distinct functions might crosstalk is unknown. It is conceivable that the regulation of intracellular iron concentrations needs to be coordinated with features of DNA metabolism; namely replication and transcription. In this context, it should be noted that many enzymes involved in DNA replication contain iron and that, during DNA

(E) AST and ALT levels in WT (+/+) and NCOA4-null (−/−) mice subjected to a hyperferric diet for 1 month (**$p < 0.01$).
(F) Representative H&E staining of liver sections from WT (+/+) and NCOA4-null (−/−) mice subjected to a hyperferric diet for 2 months.
(G) Kaplan-Meier survival curve of ten WT (+/+) (two females and eight males) and ten NCOA4-null (−/−) (two females and eight males) 4-week-old mice subjected to a hyperferric diet (2 g Fe/kg of food).

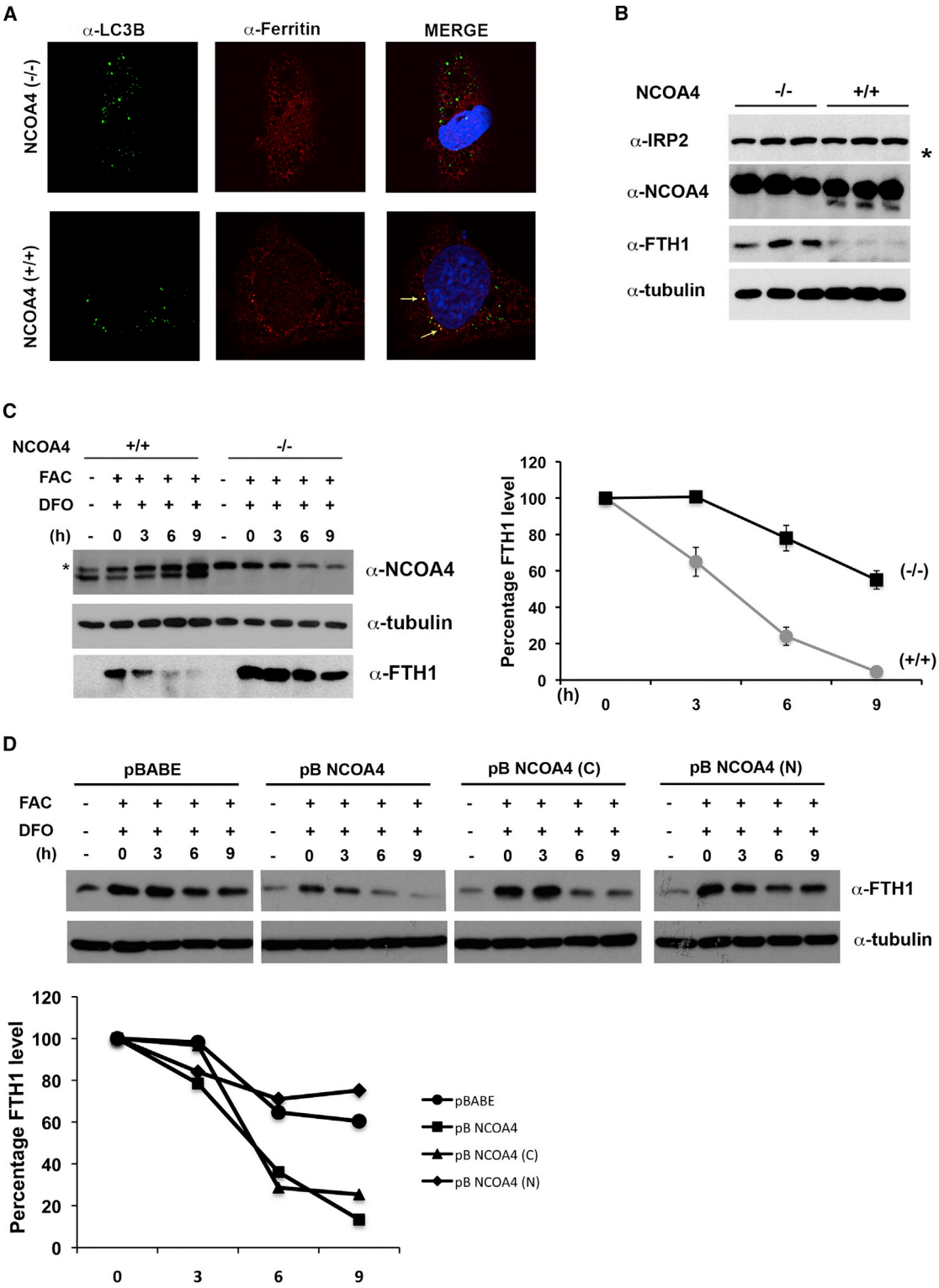

Figure 4. NCOA4-Null MEFs Show Defective Ferritinophagy

(A) Immunofluorescence analysis of LC3B (green) and Ferritin (red) co-localization in NCOA4 WT (+/+) and NCOA4-null (−/−) cells treated with chloroquine. Arrows indicate co-localization in merged images.

(B) Western blot analysis of IRP2, NCOA4, and FTH1 expression in three different WT (+/+) and NCOA4-null (−/−) MEF clones. The asterisk indicates an unspecific band. Tubulin was used as a loading control.

(legend continued on next page)

and RNA synthesis, the double helix is more sensitive to oxidative damage, being less sheltered by chromatin proteins. In addition, erythropoiesis has been linked directly to iron availability. Indeed, iron deficiency blocks erythrocyte production (Kim and Nemeth, 2015). Our data suggest that NCOA4 might be involved in coupling the proliferation of erythroblasts with iron availability so that, under conditions of iron depletion, the lack of NCOA4 results in severe impairment of erythropoiesis.

EXPERIMENTAL PROCEDURES

NCOA4$^{-/-}$ Mice

Generation of NCOA4$^{-/-}$ mice is described in Bellelli et al. (2014).

Details about animal care and management are provided in the Supplemental Experimental Procedures.

Cell Culture

WT and NCOA4-null MEFs were produced and cultured as described by Bellelli et al. (2014). HeLa cells were cultured in DMEM supplemented with 10% fetal bovine serum (FBS), 50 μg/ml penicillin-streptomycin, and 2 mM L-glutamine. To induce iron-replete conditions, MEFs were treated with 10 μg/ml of ferrum ammonium citrate (FAC), whereas, for growth under iron-deficient conditions, cells incubated for 24 hr in FAC were released in normal medium containing 50 μM deferoxamine (DFO). Chloroquine (Sigma-Aldrich) was used at a final concentration of 25 μM.

Histology

Formalin-fixed, paraffin-embedded (FFPE) sections (5 μm thick) were stained with H&E by conventional methods or deparaffinized and rehydrated by passages through xylene and alcohol series for Perl's Prussian blue or immunohistochemical (IHC) staining. The IHC staining protocol is described in the Supplemental Experimental Procedures.

Hematological Parameters and Red Cell Indices

Blood was collected by retro-orbital venipuncture in anesthetized mice using heparinized microcapillary tubes. Hematological parameters were evaluated on a Bayer Technicon Analyzer ADVIA. Hematocrit and hemoglobin were determined manually as described previously (Franco et al., 2014). Blood smears were stained with May-Grünwald-Giemsa (Sigma-Aldrich) for morphological analysis. Images were captured using a Nikon EclipseE600 microscope.

Flow Cytometric Analysis of Mouse Bone Marrow and Spleen Precursors

Flow cytometric analysis of erythroid precursors from mouse bone marrow was carried out as described by Liu et al. (2013). The cell staining and analysis procedures are reported in the Supplemental Experimental Procedures.

RNA Extraction and RT-PCR

RNA was isolated from snap-frozen mouse tissues by using TRIzol reagent (Invitrogen) and purified with the RNeasy purification kit (QIAGEN). RNA (1 μg) was reverse-transcribed with a Quantitec reverse transcription kit (QIAGEN). qRT-PCR reactions were done in triplicate, and fold changes were calculated with the following formula: $2^{-(\text{sample 1 }\Delta Ct\ -\ \text{sample 2 }\Delta Ct)}$, where ΔCt is the difference between the amplification fluorescence threshold of the mRNA of interest and the mRNA of the β-actin used as an internal reference. The primer sequences used for qPCR are available upon request.

Protein Studies

Details regarding the preparation of protein cell lysates, immunoprecipitation, and western blotting can be found in the Supplemental Experimental Procedures. Densitometric analysis of signal was performed using ImageQuant.

Antibodies

Anti-IRP2 antibody was from Santa Cruz Biotechnology. Anti-FTH1, anti-MAPK, and anti-pMAPK were from Cell Signaling Technology, and anti-transferrin receptor was from Invitrogen. Anti-FPN for IHC was from Alpha Diagnostics International, and anti-HIF2α was from Novus Biologicals. Anti-tubulin was from Sigma-Aldrich. Anti-NCOA4 is an affinity-purified rabbit polyclonal antibody raised against the C-terminal protein fragment of human NCOA4 (amino acids 239–614) (Bellelli et al., 2014). Secondary antibodies coupled to horseradish peroxidase were from Santa Cruz Biotechnology.

Tissue and Serum Iron Determination

For iron concentration measurements, mouse spleen and liver tissues were dried overnight at 110°C, dissociated mechanically, weighed, and digested in 1 ml of 3M HCl and 0.6 M trichloroacetic acid for 20 hr at 65°C. The total non-heme iron content was then measured using the bathophenanthroline method as described by Torrance and Bothwell (1968). Serum iron and transferrin saturation (the ratio of serum iron and total iron binding capacity) were calculated using the serum iron/unsaturated iron binding capacity (UIBC) and the total iron binding capacity (TIBC) kits (Randox Laboratories) according to the manufacturer's instructions.

Transduction of Retrovirus-Mediated MEFs

pBABE Puro NCOA4, NCOA4 (N), and NCOA4 (C) or the empty vector were transfected into Phoenix-eco cells, and, 48 hr later, viral supernatants were harvested and used to infect primary NCOA4-null MEFs. Forty-eight hours after infection, cells were selected with Puromycin (2.5 mg/ml) and used to analyze ferritin accumulation and degradation upon FAC treatment and release in DFO, as reported under Cell Culture.

Immunofluorescence Staining

For indirect immunofluorescence, cells were fixed in 4% paraformaldehyde, permeabilized with 0.2% Triton X-100 (5 min on ice), and then incubated with the appropriate antibodies. The immunofluorescence staining procedure is reported in the Supplemental Experimental Procedures.

Recombinant Proteins

NUS-NCOA4, NUS-NCOA4(N), and NUS-NCOA4(C) recombinant proteins were generated as described by Bellelli et al. (2014) and produced in *Escherichia coli* using standard protocols. GST-GABARAP, GST-GABARAPL1, and GST-LC3B recombinant proteins are described by Colecchia et al. (2012).

Statistics

Two-tailed unpaired Student's t test was used for statistical analysis. All p values were two-sided, and differences were considered significant when p was less than 0.05. All statistical analyses were carried out using GraphPad Instat software (version 3.06.3).

(C) Left: western blot analysis of FTH1 in WT (+/+) and NCOA4-null (−/−) cells under iron-depleted conditions. Cells were incubated for 24 hr with FAC and then released at the reported time points in medium containing the iron chelator DFO. NCOA4 and tubulin western blots are shown. The asterisk indicates an unspecific band. Right: curves showing FTH1 degradation kinetics in WT (+/+) and NCOA4-null (−/−) MEFs. Values are represented as the mean ± SD of three experiments performed in triplicate.

(D) Top: western blot analysis of FTH1 degradation in primary NCOA4-null MEFs infected with retrovirus expressing empty vector (pBABE), NCOA4 WT (pB NCOA4), or the C-terminal (pB NCOA4 (C)) or N-terminal (pB NCOA4 (N)) NCOA4 deletion mutants. Bottom: FTH1 degradation kinetics in NCOA4-null MEFs infected with the described constructs. The percentage of protein levels compared with the control was measured by densitometric analysis using ImageQuant. See also Figure S5.

SUPPLEMENTAL INFORMATION

Supplemental Information includes Supplemental Experimental Procedures and five figures and can be found with this article online at http://dx.doi.org/10.1016/j.celrep.2015.12.065.

AUTHOR CONTRIBUTIONS

Conceptualization and Design, R.B., F.C., and M.S.; Investigation, R.B., G.F., A.M., D.C., M.C., and L.D.F.; Formal Analysis, R.B., F.C., M.S., M.C., A.I., and L.D.F.; Resources, A.I., M.C., M.S., and L.D.F.; Writing, F.C., M.S., and L.D.F.

ACKNOWLEDGMENTS

We thank Nina A. Dathan for providing NCOA4 recombinant proteins. We also thank Clara Camaschella and Laura Silvestri for useful discussions and Giancarlo Troncone and Antonino Iaccarino for technical support in the IHC studies. We are grateful to Jean Ann Gilder (Scientific Communication) for editing of the text. This study was funded by the Associazione Italiana per la Ricerca sul Cancro (AIRC), by MOVIE and OCKEY grants from the Regione Campania, and by a CREME grant from the Ministero dell'Istruzione dell'Università e della Ricerca (MIUR).

Received: August 14, 2015
Revised: October 31, 2015
Accepted: December 13, 2015
Published: January 14, 2016

REFERENCES

Andrews, N.C., and Schmidt, P.J. (2007). Iron homeostasis. Annu. Rev. Physiol. *69*, 69–85.

Arosio, P., Ingrassia, R., and Cavadini, P. (2009). Ferritins: a family of molecules for iron storage, antioxidation and more. Biochim. Biophys. Acta *1790*, 589–599.

Babitt, J.L., Huang, F.W., Wrighting, D.M., Xia, Y., Sidis, Y., Samad, T.A., Campagna, J.A., Chung, R.T., Schneyer, A.L., Woolf, C.J., et al. (2006). Bone morphogenetic protein signaling by hemojuvelin regulates hepcidin expression. Nat. Genet. *38*, 531–539.

Bekker-Jensen, S., Rendtlew Danielsen, J., Fugger, K., Gromova, I., Nerstedt, A., Lukas, C., Bartek, J., Lukas, J., and Mailand, N. (2010). HERC2 coordinates ubiquitin-dependent assembly of DNA repair factors on damaged chromosomes. Nat. Cell Biol. *12*, 80–86, 1–12.

Bellelli, R., Castellone, M.D., Guida, T., Limongello, R., Dathan, N.A., Merolla, F., Cirafici, A.M., Affuso, A., Masai, H., Costanzo, V., et al. (2014). NCOA4 transcriptional coactivator inhibits activation of DNA replication origins. Mol. Cell *55*, 123–137.

Colecchia, D., Strambi, A., Sanzone, S., Iavarone, C., Rossi, M., Dall'Armi, C., Piccioni, F., Verrotti di Pianella, A., and Chiariello, M. (2012). MAPK15/ERK8 stimulates autophagy by interacting with LC3 and GABARAP proteins. Autophagy *8*, 1724–1740.

Dowdle, W.E., Nyfeler, B., Nagel, J., Elling, R.A., Liu, S., Triantafellow, E., Menon, S., Wang, Z., Honda, A., Pardee, G., et al. (2014). Selective VPS34 inhibitor blocks autophagy and uncovers a role for NCOA4 in ferritin degradation and iron homeostasis *in vivo*. Nat. Cell Biol. *16*, 1069–1079.

Fleming, R.E., and Ponka, P. (2012). Iron overload in human disease. N. Engl. J. Med. *366*, 348–359.

Franco, S.S., De Falco, L., Ghaffari, S., Brugnara, C., Sinclair, D.A., Matte', A., Iolascon, A., Mohandas, N., Bertoldi, M., An, X., et al. (2014). Resveratrol accelerates erythroid maturation by activation of FoxO3 and ameliorates anemia in beta-thalassemic mice. Haematologica *99*, 267–275.

Ganz, T., and Nemeth, E. (2012). Iron metabolism: interactions with normal and disordered erythropoiesis. Cold Spring Harb. Perspect. Med. *2*, a011668.

Heinlein, C.A., Ting, H.J., Yeh, S., and Chang, C. (1999). Identification of ARA70 as a ligand-enhanced coactivator for the peroxisome proliferator-activated receptor gamma. J. Biol. Chem. *274*, 16147–16152.

Hentze, M.W., Muckenthaler, M.U., Galy, B., and Camaschella, C. (2010). Two to tango: regulation of Mammalian iron metabolism. Cell *142*, 24–38.

Iolascon, A., d'Apolito, M., Servedio, V., Cimmino, F., Piga, A., and Camaschella, C. (2006). Microcytic anemia and hepatic iron overload in a child with compound heterozygous mutations in DMT1 (SCL11A2). Blood *107*, 349–354.

Izawa, N., Wu, W., Sato, K., Nishikawa, H., Kato, A., Boku, N., Itoh, F., and Ohta, T. (2011). HERC2 Interacts with Claspin and regulates DNA origin firing and replication fork progression. Cancer Res. *71*, 5621–5625.

Kim, A., and Nemeth, E. (2015). New insights into iron regulation and erythropoiesis. Curr. Opin. Hematol. *22*, 199–205.

Klionsky, D.J., Abdalla, F.C., Abeliovich, H., Abraham, R.T., Acevedo-Arozena, A., Adeli, K., Agholme, L., Agnello, M., Agostinis, P., Aguirre-Ghiso, J.A., et al. (2012). Guidelines for the use and interpretation of assays for monitoring autophagy. Autophagy *8*, 445–544.

Lanzino, M., De Amicis, F., McPhaul, M.J., Marsico, S., Panno, M.L., and Andò, S. (2005). Endogenous coactivator ARA70 interacts with estrogen receptor alpha (ERalpha) and modulates the functional ERalpha/androgen receptor interplay in MCF-7 cells. J. Biol. Chem. *280*, 20421–20430.

Liu, J., Zhang, J., Ginzburg, Y., Li, H., Xue, F., De Franceschi, L., Chasis, J.A., Mohandas, N., and An, X. (2013). Quantitative analysis of murine terminal erythroid differentiation in vivo: novel method to study normal and disordered erythropoiesis. Blood *121*, e43–e49.

Mancias, J.D., Wang, X., Gygi, S.P., Harper, J.W., and Kimmelman, A.C. (2014). Quantitative proteomics identifies NCOA4 as the cargo receptor mediating ferritinophagy. Nature *509*, 105–109.

Mancias, J.D., Pontano Vaites, L., Nissim, S., Biancur, D.E., Kim, A.J., Wang, X., Liu, Y., Goessling, W., Kimmelman, A.C., and Harper, J.W. (2015). Ferritinophagy via NCOA4 is required for erythropoiesis and is regulated by iron dependent HERC2-mediated proteolysis. eLife *4*, 4.

Mastrogiannaki, M., Matak, P., Keith, B., Simon, M.C., Vaulont, S., and Peyssonnaux, C. (2009). HIF-2alpha, but not HIF-1alpha, promotes iron absorption in mice. J. Clin. Invest. *119*, 1159–1166.

Nai, A., Lidonnici, M.R., Rausa, M., Mandelli, G., Pagani, A., Silvestri, L., Ferrari, G., and Camaschella, C. (2015). The second transferrin receptor regulates red blood cell production in mice. Blood *125*, 1170–1179.

Papanikolaou, G., and Pantopoulos, K. (2005). Iron metabolism and toxicity. Toxicol. Appl. Pharmacol. *202*, 199–211.

Torrance, J.D., and Bothwell, T.H. (1968). A simple technique for measuring storage iron concentrations in formalinised liver samples. S. Afr. J. Med. Sci. *33*, 9–11.

Vanoaica, L., Darshan, D., Richman, L., Schümann, K., and Kühn, L.C. (2010). Intestinal ferritin H is required for an accurate control of iron absorption. Cell Metab. *12*, 273–282.

Weber, G.J., Choe, S.E., Dooley, K.A., Paffett-Lugassy, N.N., Zhou, Y., and Zon, L.I. (2005). Mutant-specific gene programs in the zebrafish. Blood *106*, 521–530.

Yeh, S., and Chang, C. (1996). Cloning and characterization of a specific coactivator, ARA70, for the androgen receptor in human prostate cells. Proc. Natl. Acad. Sci. USA *93*, 5517–5521.

Zhang, D.L., Ghosh, M.C., and Rouault, T.A. (2014). The physiological functions of iron regulatory proteins in iron homeostasis - an update. Front. Pharmacol. *5*, 124.

Zhao, N., Zhang, A.S., and Enns, C.A. (2013). Iron regulation by hepcidin. J. Clin. Invest. *123*, 2337–2343.